M. Hong[1]
D. Isailovic[1]
R.A. McMillan[2]
V.P. Conticello[2]
[1] *Department of Chemistry, Iowa State University, Ames, IA 50011*

[2] *Department of Chemistry, Emory University, Atlanta, GA 30322*

Received 16 May 2002; accepted 11 March 2003

Structure of an Elastin-Mimetic Polypeptide by Solid-State NMR Chemical Shift Analysis

Abstract: *The conformation of an elastin-mimetic recombinant protein, $[(VPGVG)_4(VPGKG)]_{39}$, is investigated using solid-state NMR spectroscopy. The protein is extensively labeled with ^{13}C and ^{15}N, and two-dimensional ^{13}C-^{13}C and ^{15}N-^{13}C correlation experiments were carried out to resolve and assign the isotropic chemical shifts of the various sites. The Pro ^{15}N, $^{13}C\alpha$, and $^{13}C\beta$ isotropic shifts, and the Gly-3 $C\alpha$ isotropic and anisotropic chemical shifts support the predominance of type-II β-turn structure at the Pro-Gly pair but reject a type-I β-turn. The Val-1 preceding Pro adopts mostly β-sheet torsion angles, while the Val-4 chemical shifts are intermediate between those of helix and sheet. The protein exhibits a significant conformational distribution, shown by the broad line widths of the ^{15}N and ^{13}C spectra. The average chemical shifts of the solid protein are similar to the values in solution, suggesting that the low-hydration polypeptide maintains the same conformation as in solution. The ability to measure these conformational restraints by solid-state NMR opens the possibility of determining the detailed structure of this class of fibrous proteins through torsion angles and distances.* © 2003 Wiley Periodicals, Inc. Biopolymers 70: 158–168, 2003

Keywords: *chemical shift; elastin; protein conformation solid-state NMR*

INTRODUCTION

Elastin is the main structural protein responsible for the elasticity of soft tissues such as blood vessels, lung, and skin. Abnormality of elastin fibers is the cause of many disorders of the arteries and connective tissues. Elastin is formed from its soluble precursor, tropoelastin, which is dominated by hydrophobic

Correspondence to: Mei Hong; email: mhong@iastate.edu
Contract grant sponsor: Biotechnology Council
Contract grant sponsor: Iowa State University
Contract grant sponsor: Research Corporation (M. H.)
Contract grant sponsor: National Science Foundation; Contract grant number: MCB-0093398 (M. H.)
Biopolymers, Vol. 70, 158–168 (2003)

amino acids such as glycine (G), alanine (A), proline (P), and valine (V). During elastogenesis, tropoelastin molecules are covalently crosslinked through the lysine (K) residues to form mature elastic fibers.[1] Due to the insolubility of mature elastin fiber, the three-dimensional high-resolution structure of this protein still remains elusive,[1,2] thus limiting the understanding of the structure-elasticity relationship of this protein. To circumvent this problem, various synthetic peptides and polypeptides mimicking the amino acid sequence of native elastin have been designed and studied using spectroscopic and biophysical methods. One of the most common repeat sequences is VPGVG, which is found between the lysine crosslinks of bovine and porcine elastin.[2] Poly(VPGVG) and shorter peptides with the same repeat motif have been investigated by Raman and infrared spectroscopy,[3] circular dichroism (CD),[4,5] solution nuclear magnetic resonance (NMR),[6] X-ray diffraction,[7] and molecular dynamics simulations.[8] These studies are overall consistent with the formation of a β-turn structure around the Pro-Gly pair, supporting a model that the polypeptide forms a β-spiral structure.[9,10]

However, most studies of the molecular structure of the elastin-mimetic peptides and proteins were conducted in organic or aqueous solutions, despite the fact that natural elastin is amorphous and insoluble. Solid-state NMR spectroscopy provides a powerful tool for determining molecular distances, torsion angles, and conformational distributions of solid proteins directly in their native environment. High-resolution solid-state NMR spectra can be obtained by spinning the protein sample around an axis tilted at the magic angle (54.7°) with respect to the magnetic field. This can be combined with isotopic (^{13}C and ^{15}N) labeling to characterize the structure of medium to large fibrous proteins such as silk and collagen.[11–14]

Recently, a new elastin-mimetic recombinant polypeptide, $[(VPGVG)_4(VPGKG)]_{39}$, termed poly(Lys-25), was synthesized and found to exhibit similar mechanical properties to those of the native elastin.[15] For example, the hydrated poly(Lys-25) shows an inverse temperature transition, where the volume of the protein decreases upon heating, to a gel state called coacervate. The phase-transition temperature depends on the pH and ionic strength of the solution. The protein also exhibits a beaded filamentous network morphology characteristic of natural elastin.[16] Thus, poly(Lys-25) provides an excellent model system for native elastin. The ability to synthesize an environmentally responsive elastic protein in large quantities permits the possibility of engineering artificial tissues and drug delivery devices with desired elastic properties. It also allows tailored isotopic labeling schemes to be used to facilitate solid-state NMR characterization of the protein structure on the molecular level.

In this article, we report an initial study of the conformation of solid poly(Lys-25) using magic-angle spinning (MAS) NMR spectroscopy. Specifically, we have determined the isotropic and anisotropic chemical shifts of various ^{13}C and ^{15}N sites to provide conformational constraints of the protein below the inverse temperature transition. Nuclear spin chemical shift is a sensitive probe of the secondary structure of proteins.[17–19] The local torsion angles exert a dominant influence on the backbone ^{13}C and ^{15}N chemical shielding of amino acid residues. Conformation-dependent ^{13}C and ^{15}N isotropic chemical shifts of proteins in solution and in the solid state have been compiled based on NMR-determined protein structures [11,19–21]. These have yielded empirical isotropic shift surfaces, which can be used to predict the conformation of amorphous proteins whose high-resolution structure is unknown. In addition to isotropic chemical shifts, anisotropic chemical shifts also depend on the secondary structure, as shown by quantum chemical calculations and solid-state and solution NMR experiments [22–26]. In this work, we have measured the ^{13}C and ^{15}N chemical shifts of poly(Lys-25) on a ^{13}C and ^{15}N labeled sample using 2D homo- and heteronuclear NMR techniques. Our results support a type-II β-turn conformation at the Pro-Gly position in the polypeptide repeat sequence. Isotopic labeling not only enhanced the sensitivity of the experiments but also allowed multiple chemical shift restraints to be obtained using only one sample.

MATERIALS AND METHODS

Poly(Lys-25) has an amino acid sequence of $[(VPGVG)_4(VPGKG)]_{39}$ and a molecular weight of approximately 81 kDa. It was cloned and expressed in M9 media as described previously.[15] For ^{13}C and ^{15}N labeling, the sole carbon source in the M9 media was [2-^{13}C] labeled glycerol, while the nitrogen source was ^{15}N-labeled ammonium sulfate. It has been demonstrated on ubiquitin and α-spectrin SH3 domain that the singly ^{13}C labeled glycerol gives rise to selectively labeled proteins due to the specificity of the amino acid biosynthetic pathways.[27–29] For poly(Lys-25), the ^{13}C-labeled sites are Val Cα and Cβ, Gly Cα, Pro Cα, Cβ, Cδ, and CO, Lys Cα, Cγ, Cδ, and Cϵ. Thus, neglecting the low-abundance Lys residues (4 mol %), the unlabeled carbon sites are Pro Cγ, Val Cγ, and the CO of Val and Gly. About 7.8 mg of lyophilized protein was packed into a 4 mm zirconium rotor and then hydrated by direct addition of 2 μL of deionized water to achieve better homogeneity and narrower line widths. Further hydration

did not improve the line widths of the spectra but reduced the sensitivity due to excessive molecular motion.

NMR spectra were recorded on a Bruker DSX-400 spectrometer (Karlsruhe, Germany) operating at a magnetic field of 9.4 tesla, which corresponds to a resonance frequency of 100.72 MHz for ^{13}C and 40.59 MHz for ^{15}N. A triple-resonance MAS probe equipped with a 4 mm spinning module was used. Typical radio frequency (rf) field strengths for the ^{1}H channel were 85 kHz for decoupling and 50 kHz for cross polarization (CP). Carbon and nitrogen 90° pulse lengths were about 5 and 6 μs, respectively. Spinning speeds of 5–7 kHz were used for most experiments. All experiments were conducted at 293 ± 2 K.

A 2D ^{13}C homonuclear double-quantum (DQ) correlation experiment was carried out using a previously described pulse sequence.[30] Briefly, after cross polarization from ^{1}H to ^{13}C, DQ coherence between spatially close ^{13}C spins was generated using the CMR7 sequence,[31] which recouples homonuclear dipolar couplings under MAS. Eight rotor periods of CMR7 recoupling were applied under a spinning speed of 6 kHz, giving rise to a DQ excitation time of 1.33 ms. This allowed the detection of correlation peaks between remote ^{13}C spins. The DQ coherence evolves during the t_1 period so that the sum chemical shift of the two coupled spins is encoded. It is then reconverted to single-quantum magnetization and detected during the t_2 period. One hundred t_1 slices, corresponding to a maximum DQ evolution time of 2.4 ms, were acquired. The 2D experiment took about 12 h.

Two-dimensional ^{15}N-^{13}C heteronuclear correlation (HETCOR) spectra were acquired using a previously described sequence,[32,33] in which polarization transfer between ^{13}C and ^{15}N spins was achieved in a heteronuclear single-quantum coherence fashion with REDOR as the mixing sequence.[34] After initial cross polarization from ^{1}H to ^{13}C, a REDOR mixing period is applied that involves ^{15}N 180° pulses spaced half a rotor period apart and a single ^{13}C 180° pulse in the middle. This creates ^{13}C antiphase magnetization of the type C_xN_z. This is followed by a pair of ^{13}C and ^{15}N 90° pulses, which converts the spin operator to ^{15}N magnetization N_xC_z. This single-quantum ^{15}N magnetization evolves under the ^{15}N isotropic chemical shift interaction for a period t_1. At the end of the evolution period, the ^{15}N magnetization is reconverted to observable ^{13}C magnetization using the same pair of 90° pulses and an identical ^{13}C-^{15}N REDOR period. The REDOR mixing time is varied to maximize the intensities of either cross peaks between directly bonded spins or cross peaks between spins separated by multiple bonds. Sixty-four t_1 slices were collected for the ^{15}N dimension, resulting in a maximum t_1 evolution time of 4.6 ms. The acquisition time for each 2D spectrum was 3–5 h.

The chemical shift anisotropy (CSA) patterns of ^{13}C and ^{15}N sites were recoupled under MAS using the recently developed SUPER sequence.[35] This experiment yielded static-like chemical shift powder patterns under MAS by recoupling the CSA interaction with rotor-synchronized 360° pulses. The timing of the 360° pulses was chosen to give a CSA scaling factor of 0.155.[36] Slow spinning speeds of 2.5–3 kHz were used for these experiments.

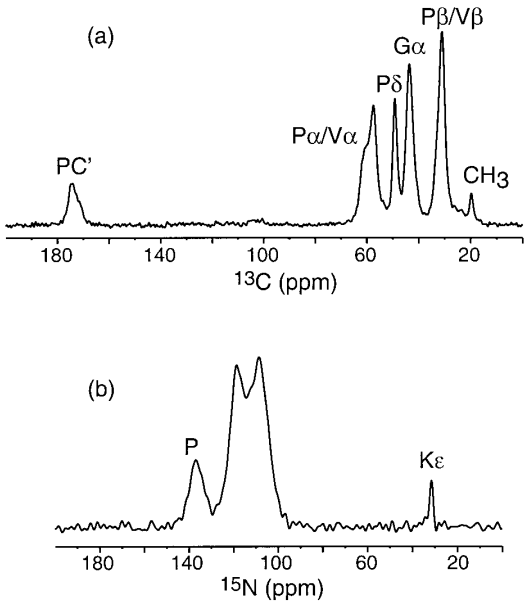

FIGURE 1 (a) ^{13}C spectrum of poly(Lys-25). (b) ^{15}N spectrum of poly(Lys-25). Both were obtained under 7 kHz of MAS. Peak overlap is present in both spectra.

The ^{13}C chemical shifts were referenced to TMS indirectly through the carbonyl carbon of [1-^{13}C] glycine (176.4 ppm). The ^{15}N chemical shifts were referenced to liquid ammonia indirectly through the sidechain ^{15}N signal of uniformly labeled glutamine (38.4 ppm).

RESULTS

^{13}C and ^{15}N Isotropic Chemical Shifts

Figure 1 shows the 1D ^{13}C and ^{15}N CP-MAS spectra of selectively and extensively ^{13}C-labeled and uniformly ^{15}N-labeled poly(Lys-25). The protein was hydrated to 20% by weight, which narrowed the ^{15}N lines by 1.1–2.5 ppm and ^{13}C lines by about 0.5 ppm compared to the lyophilized sample. Despite this resolution improvement, substantial resonance overlap remained in the 1D spectra. For example, in the ^{13}C spectrum, the most downfield Cα peak at 57–62 ppm is a superposition of at least two resonances. Based on the characteristic ^{13}C chemical shifts of amino acids, we can tentatively assign this broad peak to Val and Pro Cα, but the exact assignment of the underlying peaks can only be made from 2D correlation spectra. Similarly, the peak at 30 ppm can be tentatively

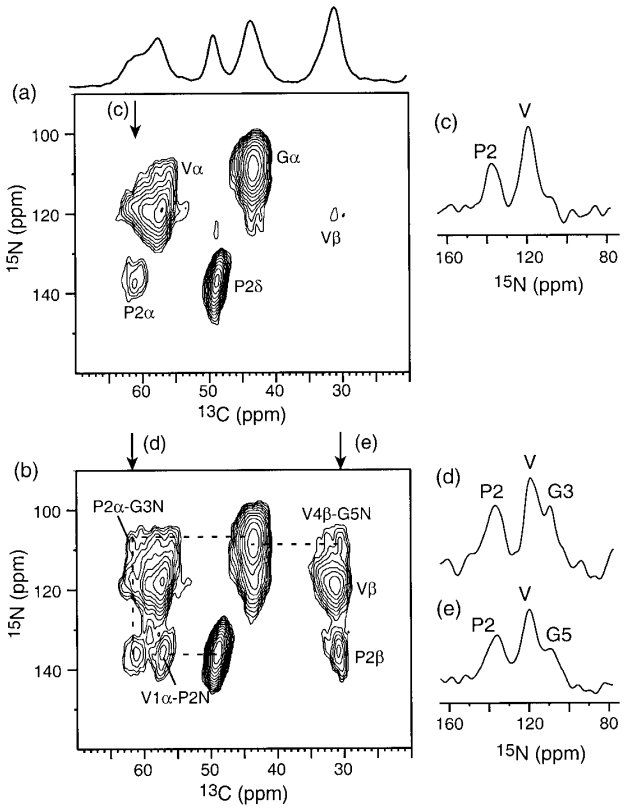

FIGURE 2 Two-dimensional ^{15}N-^{13}C correlation spectra of poly(Lys-25) with different ^{15}N-^{13}C mixing times. (a) Mixing time = 0.86 ms. Mostly directly bonded ^{13}C-^{15}N spin pairs are detected. (b) Mixing time = 2.29 ms. Two- and three-bond connectivities are observed. The spectra were acquired under 7 kHz of MAS. (c–e) ^{15}N cross sections at ^{13}C frequencies indicated by arrows.

assigned to Val and Pro Cβ without resolution. The selectivity of the ^{13}C labeling pattern is manifested by the complete lack of a Pro Cγ signal near 25 ppm and the nearly complete suppression of the Val Cγ methyl signal at 19 ppm. In the ^{15}N spectrum, the most upfield signal at 33.6 ppm can be readily assigned to the Lys sidechain NH_3 group, while the most downfield signal at 137 ppm can be attributed to the unprotonated Pro ^{15}N. However, this still leaves the two broad peaks between 100 and 120 ppm as the four Val and Gly ^{15}N amides without clear separation.

To resolve the overlapping resonances, we carried out 2D ^{15}N-^{13}C HETCOR experiments. With a short mixing time of 0.86 ms, the HETCOR spectrum (Figure 2a) showed mostly one-bond ^{15}N-^{13}C correlation peaks. In the aliphatic ^{13}C region, this corresponds to intraresidue ^{15}N-^{13}Cα peaks. These immediately confirmed several tentative assignments made in the 1D spectra. For example, the intensities at the ^{15}N chemical shift of 137 ppm can be definitively assigned to Pro, because Pro is the only residue whose ^{15}N spin is directly bonded to two ^{13}C spins, Cα and Cδ. The identification of Pro ^{15}N assigns the Pro ^{13}Cα chemical shift to be 60.8 ppm. Thus, the downfield shoulder of the ^{13}C peak around 60 ppm in the 1D spectrum is partly attributed to Pro Cα. The broad resonance at (^{15}N, ^{13}C) frequencies of (109 ppm, 43.3 ppm) is unmistakably Gly, because both ^{13}Cα and ^{15}N chemical shifts of Gly are usually upfield from other amino acids.

When the ^{15}N-^{13}C polarization-transfer time was increased to 2.29 ms (Figure 2b), ^{15}N and ^{13}C spins that are separated by more than one bond were also detected. The most useful connectivities are interresidue ones such as $C\alpha_{i-1} - N_i$. For example, a clear peak at (137 ppm, 57 ppm) can be assigned to the Val-1 Cα and Pro-2 ^{15}N correlation due to the characteristic Pro ^{15}N chemical shift and the absence of

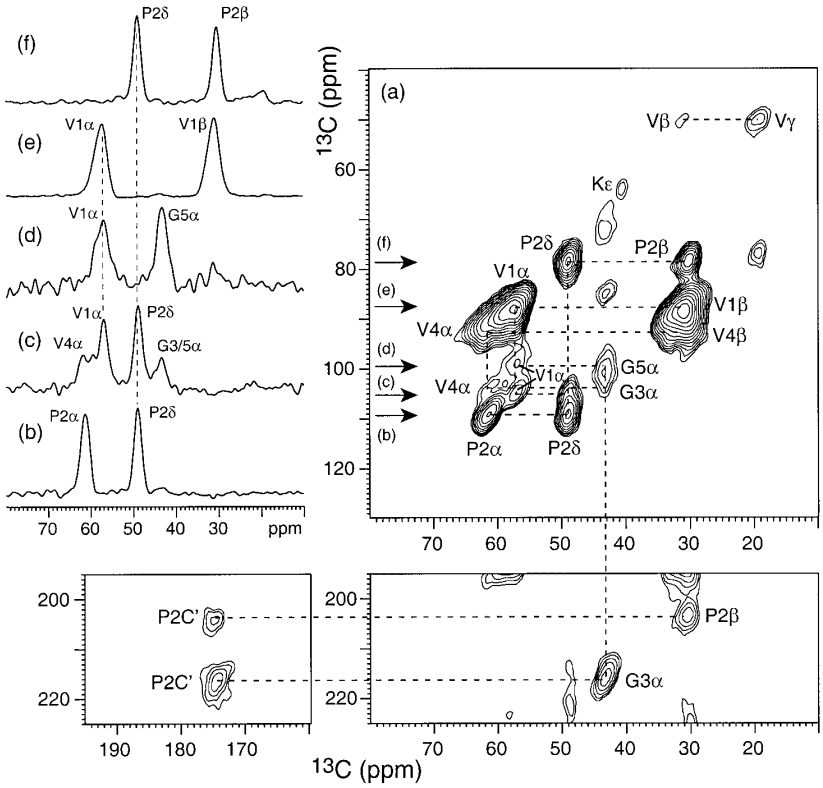

FIGURE 3 (a) Two-dimensional ^{13}C-^{13}C double-quantum correlation spectrum of poly(Lys-25), obtained with a double-quantum excitation time of 1.33 ms and under a spinning speed of 6 kHz. (b–f) Cross sections at ω_1 frequencies indicated by the arrows.

this peak in the short mixing time spectrum. This unambiguously identifies Val-1 Cα as the upfield component of the broad peak in the 1D spectrum (Figure 1a). By similar arguments, we can assign the Pro-2 Cα – Gly-3 ^{15}N correlation, and the Val-4 Cβ and Gly-5 ^{15}N cross peak. Also observed in the spectrum are intraresidue two-bond correlation peaks, such as between Pro-2 Cβ and Pro-2 ^{15}N, and between Val ^{15}N and Val $^{13}C\beta$. A few representative ^{15}N cross sections are extracted from the 2D spectra and shown in Figure 2(c–e). To further resolve the remaining overlapping resonances, we measured the 2D ^{13}C-^{13}C DQ correlation spectrum of poly(Lys-25) (Figure 3). The DQ spectrum, analogous to the liquid-state INADEQUATE spectra,[37] exhibits the signals of the coupled ^{13}C spins at the same ω_1 frequency, which is the sum chemical shifts of the two spins. These are correlated with single-quantum ^{13}C chemical shifts of the individual sites in the direct (ω_2) dimension. Connecting the center of the pairs of signals through each ω_1 slice, we obtain a characteristic slope-2 diagonal across the 2D spectrum. For this solid-state INADEQUATE experiment to work, the coupled ^{13}C spins need not be directly bonded, because the polarization transfer mechanism is the through-space ^{13}C-^{13}C dipolar coupling rather than the through-bond scalar coupling. Thus, any spatially close ^{13}C spin pairs are detected. At the double-quantum excitation time (1.33 ms) used, the 2D spectrum exhibits a number of medium- and long-range correlation peaks in addition to the obvious one-bond signals such as Val Cα-Cβ (Figure 3e). These include two-bond intraresidue peaks such as Pro Cα–Cδ (Figure 3b) and Pro Cδ–Cβ (Figure 3f), and three-bond correlation such as between Val-1 Cα and Gly-5 Cα (Figure 3d). These long-range correlation peaks further resolved the Val-1 and Val-4 Cα signals: Val-1 Cα is correlated with Pro-2 Cδ while Val-4 Cα is coupled to the Cα of either Gly-3 or Gly-5 (Figure 3c). Finally, the Gly-3 Cα is unambiguously assigned by its correlation with Pro-2 C$'$, which is the only labeled carbonyl carbon in the polypeptide. Several 1D cross sections are ex-

tracted to indicate the good signal-to-noise of the 2D spectrum. In fact, the 2D DQ spectrum has sufficient sensitivity to exhibit weak signals from the natural abundance Val Cγ (19 ppm), which is correlated with the labeled Val Cβ, and the signals of the Lys sidechain Cϵ (40.7 ppm) and Cγ (23.7 ppm), which are well labeled but occur infrequently in the protein. Because these side chain chemical shifts are not sensitive to the backbone conformation, they are not used in the conformation analysis below.

The resonance assignment is unaffected by possible low levels of ^{13}C scrambling, because only frequency information and not intensities are sought after. Moreover, the amino acid sequence of the protein is simple enough and the number of chemically unique carbons is small enough that there are few possibilities for scrambling to chemically distinct carbons that may overlap with the signals of the labeled sites. Instead, the selective ^{13}C labeling is applied mainly to reduce line broadening that results from multispin homonuclear couplings. The choice of [2-^{13}C] glycerol instead of other singly labeled carbon precursors is appropriate for the purpose of conformational analysis because it labels all ^{13}Cα sites, whose chemical shifts are most sensitive to local torsion angles among all heavy atoms of the protein backbone. The 2D hetero- and homonuclear correlation spectra shown here resolve and assign all labeled carbon sites, especially those with nearly identical chemical shifts such as Val-1 and Val-4, and Gly-3 and Gly-5.

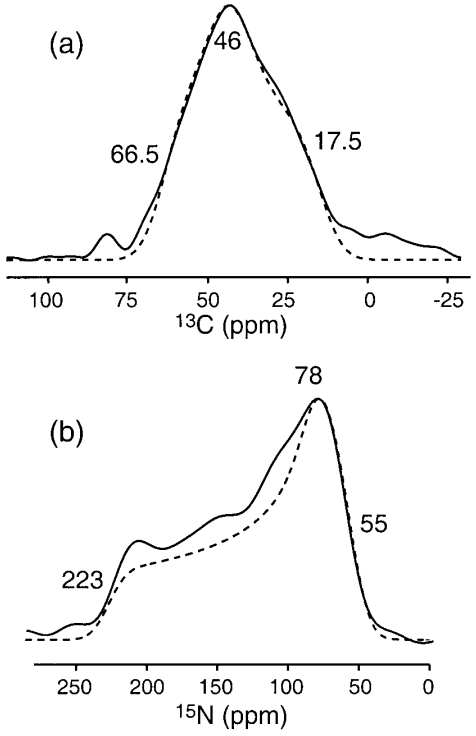

FIGURE 4 ^{13}C and ^{15}N chemical shift anisotropy spectra of (a) Gly Cα and (b) Val ^{15}N. Best fit simulations (dashed line) are superimposed with the experimental spectra (solid line).

Table I ^{13}C and ^{15}N Solid-State NMR Chemical Shifts (ppm) of Poly(Lys-25).

Residue	Cα	Cβ	^{15}N
Val-1	57.1 (−1.0)	31.3 (+0.4)	119.4 (−1.1)
Pro-2	60.8 (−0.8)	30.5 (+0.1)	136.9
Gly-3	43.3 (−0.1)	N.A.	108.9 (−0.2)
Val-4	61.5 (+1.0)	30.1 (−1.1)	119.4 (+0.2)
Gly-5	43.3 (−0.1)	N.A.	109.0 (−0.1)

Numbers in parentheses correspond to the secondary shifts, obtained using the random coil values in ref.[39]

^{13}C and ^{15}N Chemical Shift Anisotropy

The assignment of the ^{13}C and ^{15}N isotropic shifts allowed us to measure the chemical shift anisotropy of selected sites to complement the isotropic-shift information on poly(Lys-25). The CSA patterns were measured using the recently introduced 2D SUPER technique, which recouples the chemical shift anisotropy in a quasi-static fashion under MAS through 360° pulses.[35] However, these 360° recoupling pulses also reintroduce the homonuclear dipolar couplings, thus the powder patterns of ^{13}C sites with directly bonded ^{13}C neighbors are complicated by the additional ^{13}C-^{13}C dipolar coupling.[38] Thus, at this point, we only analyze the CSA patterns of isolated spins, including Gly Cα, Pro Cδ, and the backbone ^{15}N sites. Figure 4 shows the ^{13}Cα CSA spectrum of Gly (a) and the ^{15}N CSA pattern of Val ^{15}N (b). The principal values were extracted from best fits of the experimental powder patterns. The Gly Cα spectrum has an anisotropic span of $\Omega = \delta_{11} - \delta_{33} = 49$ ppm, and an asymmetry parameter $\eta = (\delta_{11} - \delta_{22})/(\delta_{33} - \delta_{iso})$ of 0.79 (Table II). Although this pattern results from a superposition of Gly-3 and Gly-5 Cα signals, the good agreement between the experimental and simulated spectra suggests that the two Gly residues have very similar CSAs.[28] The Val ^{15}N powder pattern is best fit by a span of 168 ppm and an asymmetry parameter of 0.22, which are typical for amide ^{15}N sites in proteins.

Table II ^{13}C and ^{15}N Chemical Shift Anisotropic Span (ω) and Asymmetry Parameter (η) in Poly(Lys-25)

Residue	Ω (ppm)	η
Gly-3 and Gly-5 Cα	49	0.79
Gly-3 Cα	50	0.93
Pro-2 Cδ	50	0.65
Val-1 and Val-4 ^{15}N	168	0.22
Gly-3 and Gly-5 ^{15}N	164	0.22
Pro-2 ^{15}N	185	0.89

DISCUSSION

The ^{13}C and ^{15}N resonance assignment shown above yielded the isotropic chemical shifts (δ_{exp}) for all labeled sites in poly(Lys-25), which are listed in Table I. These permit the comparison of the ^{13}C and ^{15}N isotropic shifts in poly(Lys-25) with the known conformation-dependent chemical shifts of amino acids to constrain the backbone structure of this elastin-mimetic protein. For Cα and Cβ spins, the local ϕ, ψ torsion angles are the predominant factor determining the chemical shifts. The amino-acid sequence dependence of these chemical shifts is very minor.[21] Secondary-structure dependent isotropic shifts, defined as $\delta(\phi\ \psi) = \delta_{exp} - \delta_{rc}$, where δ_{rc} is the isotropic shift of random coils, have been extensively studied and compiled based on protein structures determined using solution and solid-state NMR.[11,39,40] Cα and C$'$ carbons exhibit negative secondary shifts in the β-sheet conformation but positive secondary shifts in α-helices, while Cβ and ^{15}N secondary shifts are positive for the sheet conformation but negative in helical residues. Turn and loop structures exhibit chemical shifts close to the random coil values, except for Pro, where large positive ^{15}N secondary shifts were observed for turn structures.[17] Pro also exerts a non-negligible effect on the chemical shifts of the preceding residue, independent of the conformation.[39] Statistical analyses of the protein chemical shifts and their correlation with 3D structures have resulted in ever more detailed chemical shift surfaces as a function of the ϕ, ψ torsion angles.[21] Using these empirical chemical shift surfaces, one can predict, semi-quantitatively, the torsion angle ranges of protein polymers with unknown structure such as silk[41] and collagen.[14] These empirical chemical shift surfaces have now been confirmed by quantum chemical calculations on molecular fragments consisting of an amino acid with N- and C-terminal peptide bonds but without complete flanking residues.[42] These calculations, which yield the complete chemical shift tensor principal axes orientations and magnitudes,[22,23,43] show without a doubt that the chemical shifts of α carbons are primarily determined by local Ramachandran angles, and are little affected by the type of neighboring residues.[44] In the following, we use the residue-specific empirical isotropic chemical shift surfaces to analyze the isotropic shifts measured in poly(Lys-25), and the *ab initio* calculated anisotropic chemical shifts to analyze the experimental Gly Cα CSA.

To obtain the secondary shifts of poly(Lys-25), one must specify the random-coil chemical shift values. We use the random coil ^{13}C and ^{15}N shifts from Wishart et al.,[39] in which the ^{13}C chemical shifts were referenced to internal DSS. These were converted to chemical shifts relative to TMS by subtracting 1.7 ppm.[45] Table I compiles the experimental secondary shifts for Cα, Cβ, and ^{15}N of $(VPGVG)_n$. Their comparison with the average helical and sheet secondary shifts[46] is shown in Figure 5.[46]

We first analyze the chemical shifts of Pro-2 and Gly-3, which were postulated to form the central two residues, i+1 and i+2, respectively, of a β-turn under suitable hydration, temperature, and pH conditions.[10] The Pro Cα isotropic shift corresponds to a secondary shift of -0.8 ppm. This differs significantly from the helical value of $+2.2$ ppm, thus ruling out the helical structure. More specifically, using the Pro Cα isotropic shielding surface constructed by Iwadate and coworkers,[21] we find that the experimental value corresponds to ϕ torsion angles of -80 to $-110°$ and ψ angles between 90 and 180° (Figure 6a, shaded area). This is roughly consistent with the torsion angles for the i+1 residue of type-II β-turn ($\phi = -60°$, $\psi = 120°$), but rejects the type-I β-turn conformation ($\phi = -60°$, $\psi = -30°$).[47] For Pro Cβ, a secondary shift of $+0.1$ ppm was found and is consistent with the conformation tendency of Pro Cα: it translates to a ϕ torsion angle from -45 to $-100°$, and a ψ angle between 90 and 170°. The secondary shift of Gly Cα is -0.1 ppm. On the chemical shift surface, several torsion angle regions are consistent with this shift (Figure 6a, unfilled areas), among which are the i+2 residue of both type-II β-turn ($\phi = 80°$, $\psi = 0°$) and type-I β-turn ($\phi = -80°$, $\psi = 0°$). Taken together, however, the Pro-2 and Gly-3 ^{13}C chemical shifts favor the type-II β-turn structure over a type-I β-turn.

It is also of interest to examine the local conformation of the other three residues sandwiching the Pro-Gly pair in the VPGVG sequence. Val-1 exhibits a Cα secondary shift of -1.0 ppm and a Cβ secondary shift of $+0.4$ ppm. These values were obtained after taking into account the sequence-specific effect

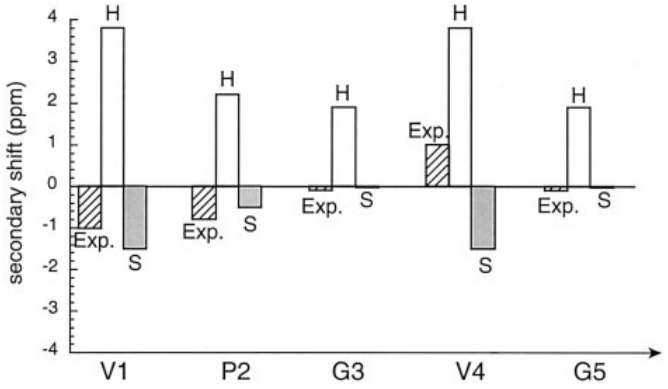

FIGURE 5 Cα secondary shifts (stripes) of the VPGVG repeat unit in poly(Lys-25), extracted from 2D solid-state NMR spectra. For comparison, the secondary shifts for helical (H, open rectangles) and sheet (S, shaded rectangles) conformations for these residues are also shown.

exerted by Pro-2.[39] The negative Cα secondary shift is comparable to the average β-sheet secondary shift for Val, indicating that Val-1 adopts β-sheet torsion angles of about $\phi = -135°$ and $\psi = 135°$. This is consistent with the quantitative ϕ torsion angle measured by correlating the N-H and Cα-Hα dipolar couplings,[48] which yielded a ϕ angle of either $-135°$ or $-105°$ (data not shown). In contrast, Val-4 displays a small positive Cα secondary shift of $+1.0$ ppm and a negative Cβ secondary shift of similar magnitude. The Cα secondary shift is small compared to the average helical secondary shift of $+3$ ppm, suggesting that Val-4 conformation is intermediate between the two canonical structures. On the chemical shift surfaces, the Val-4 chemical shifts constrain the residue to two possible (ϕ, ψ) angles: ($-90°$, $-30°$) and ($-60°$, $+120°$) (Figure 6b).

The experimental ^{15}N isotropic shifts confirm the ^{13}C-based secondary structure analysis. The strongest indication of the β-turn conformation at the Pro-Gly linkage is the Pro ^{15}N chemical shift of 136.9 ppm. This is significantly downfield from both the helical (123.2 ppm) and sheet (127.5 ppm) chemical shifts, but is consistent with the average isotropic shift of 133.6 ppm for turns.[39] Because the Pro ^{15}N chemical shift is not influenced by hydrogen bonds, its dependence on secondary structure is particularly sensitive. It is interesting to compare the Pro ^{15}N shift of this elastin-mimetic polypeptide with that of collagen triple-helix, which has torsion angles of $\phi = -80°$ and $\psi = 150°$.[47] The collagen ^{15}N isotropic shift is 130 ppm, less downfield than poly(Lys-25) but still reflecting a turn conformation.[49] Further supporting the β-turn conformation of the central Pro-Gly residue pair is the Gly-3 ^{15}N isotropic shift of 108.9 ppm, which is closer to the turn or coil value of 109.2 ppm than to either the helix (107.9 ppm) or sheet (109.7 ppm) isotropic shifts.

The typical ^{13}C and ^{15}N line widths of poly(Lys-25) are 1.5–4 ppm and 8–10 ppm, respectively. The ^{15}N line width is quite typical for amorphous proteins, while the ^{13}C line width is slightly narrower than some other fibrous proteins such as dragline spider silk[50] and Bombyx mori fibroin.[11,41,51,52]. The finite line widths indicate the presence of significant conformational distribution and solid-state packing effects, which exist even in crystalline solids with homogeneous conformation.[53] The broad ^{15}N line widths compared to ^{13}C most likely reflect heterogeneous hydrogen-bonding environments, a factor known to influence the ^{15}N chemical shifts but not Cα chemical shifts. Thus, the chemical shift analysis here, which is based on the frequency of the well-defined peak maxima, only indicates the predominant backbone conformation of the residues in the protein. Measurements of more direct conformational parameters, such as intramolecular distances and torsion angles, are necessary in order to quantify the conformational heterogeneity of this protein.

Interestingly, the ^{13}C line width is not uniform across the (VPGVG) unit. The Pro peaks are on average about 2 ppm narrower than the Val and Gly peaks, based on the 2D ^{13}C DQ spectrum and the ^{15}N-^{13}C HETCOR spectra. The differential line widths suggest that the conformation of the Pro residue is better defined than other residues in the VPGVG repeat, and that the β-turn conformation of Pro-Gly is relatively uniform throughout the protein. This is consistent with a recent circular dichroism study of VPGVG peptides of varying lengths, which

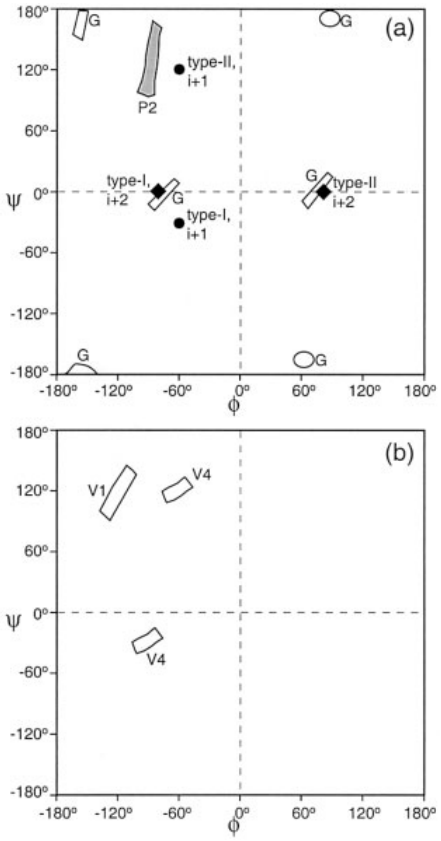

FIGURE 6 Torsion angles of the VPGVG repeat sequence, as restrained by the isotropic and anisotropic chemical shifts measured by solid-state NMR. (a) Pro (shaded area) and Gly (unfilled areas) torsion angles. The ideal torsion angles for the i+1 (solid circles) and i+2 (solid diamonds) residues of type-I and -II β-turns are indicated for comparison. Type-I β-turns can be ruled out based on the Pro chemical shifts. (b) Val-1 and Val-4 torsion angles.

found that the formation of type-II β-turn structure occurs in a single pentameric unit rather than requiring a cooperative transition of multiple pentamer units.[4]

Overall, the solid-state ^{13}C isotropic shifts of poly(Lys-25) agree well with the values found in solution,[15] indicating that the solution structure is largely maintained in the solid sample. The influence of hydration on elastin has been recently investigated using ^{13}C CP-MAS experiments.[54] At sufficiently high hydration, the protein exhibits extensive internal motion. However, the average conformation of the polypeptide chains appears to be little altered by hydration, judging from the ^{13}C chemical shifts measured in the solution study and in the solid state.

The Cα chemical shift anisotropies of Gly-3 and Gly-5 complement the isotropic shift analysis. The recoupled CSA powder pattern exhibits a span of 49 ppm and an asymmetry parameter of 0.79. These values agree with the quantum chemical calculated CSAs for both type-I and -II β-turns,[55] but are much larger than the calculated CSA values for β-sheet (32 ppm) and α-helical (34 ppm) Gly. Therefore, these two canonical conformations alone cannot be the primary structure for Gly-3 and Gly-5 in poly(Lys-25). We have recently conducted a spectroscopic filter experiment to selectively detect the Gly-3 Cα signal in the absence of Gly-5. The resulting Gly-3 Cα CSA (Ω = 50 ppm, η = 0.93) is very similar to the combined Gly-3 and Gly-5 CSA pattern measured here.[28] This suggests that the two Gly residues have similar torsion angles; however, this is not definitive, because several limited regions in the Ramachandran diagrams yield isotropic and anisotropic chemical shifts consistent with the measured Gly value (Figure 6a). These regions, located around (ϕ, ψ) angles of ($-170°$, $-160°$), (90°, 170°), and (60°, $-160°$), are rarely populated by other amino acids but are possible for the conformationally flexible Gly. Interestingly, the pair of angles ($-170°$, $-160°$) is close to the value predicted for Gly-5 in the original β-spiral model built using energy minimization.[9] More precise determination of the conformation of the Gly residues through torsion angle measurements is now underway using site-specifically labeled peptides.

The chemical shifts of poly(Lys-25) in the solid state indicate that the protein at low hydration and below the phase transition temperature has a relatively well defined turn structure centered around the Pro-Gly residue pair. This differs from the hypothesis that the protein adopts a β-spiral conformation only above the inverse temperature transition but assumes a random coil structure below it.[10] Our result suggests that the conformational tendency of the Pro ring to adopt a ϕ angle of $-60°$ and to form turn structures in conjunction with Gly is sufficiently strong that a repeating structure of β-turns may be natural for this polypeptide. Environmental factors such as temperature, hydration, and pH may affect only the percentage of β-turns but not its presence or absence. These environmental factors will also influence the dynamics of the protein, which is the topic of a separate study. The information from the solid-state NMR chemical shifts is consistent with a recent CD study of short VPGVG peptides that showed a significant amount of type-II β-turns below the phase transition temperature.[4] It is also consistent with molecular dynamics simulations that indicated 36% of β-spiral structure below the phase transition temperature.[8] The

presence of β-turn conformation below the inverse temperature transition suggests that the development of elastomeric forces observed in the high-temperature state may result more from internal dynamics of the protein rather than from significant conformational changes.

CONCLUSION

We have shown here that the measurement of isotropic and anisotropic ^{13}C and ^{15}N NMR chemical shifts restrains the conformation of the elastin-mimetic polypeptide, poly(Lys-25). Several lines of evidence, including the Pro-2 Cα, Cβ, and ^{15}N isotropic shifts, and the Gly-3 Cα isotropic and anisotropic chemical shifts, support a β-turn structure as the primary conformation of the Pro-Gly residue pair. The Pro-2 torsion angles are clearly indicative of a type-II β-turn, while Gly-3 can also adopt torsion angles other than those of a type-II β-turn. Isotropic shift surfaces as a function of Ramachandran angles were used to obtain these conformational restraints. Apart from the Pro-Gly residue pair, Val-1 adopts the β-sheet conformation, while Val-4 exhibits a conformation intermediate between α-helix and β-sheet. While these chemical shifts specify the average conformation, the broad ^{15}N and ^{13}C lines in the spectra indicate that the protein is structurally heterogeneous.

The solid-state NMR chemical shifts provide only qualitative restraints to the conformation of this elastin-mimetic protein. Deviations from the ideal type-II β-turn torsion angles, especially at the Gly-3 position, cannot yet be excluded. More detailed information on the turn structure, as well as on the conformational distribution in the protein, must come from distance and torsion angle measurements. These experiments are currently underway using more specifically labeled samples to further elucidate the structure of this elastin-mimetic protein.

This work was partially supported by a University Research Grant at Iowa State University.

REFERENCES

1. Debelle, L.; Tamburo, A. M. Int J Biochem Cell Biol 1999, 31, 261–272.
2. Gray, W. R.; Sandberg, L. B.; Foster, J. A. Nature 1973, 246, 461–466.
3. Prescott, B.; Renugopalakrishnan, V.; Thomas Jr., G. T. Biopolymers 1987, 26, 934–936.
4. Reiersen, H.; Clarke, A. R.; Rees, A. R. J Mol Biol 1998, 283, 255–264.
5. Arad, O.; Goodman, M. Biopolymers 1990, 29, 1651–1668.
6. Urry, D. W.; Chang, D. K.; Krishna, N. R.; Huang, D. H.; Trapane, T. L.; Prasad, K. U. Biopolymers 1989, 28, 819–833.
7. Cook, W. J.; Einspahr, H.; Trapane, T. L.; Urry, D. W.; Bugg, C. E. J Am Chem Soc 1980, 102, 5502–5505.
8. Li, B.; Alonso, D. O. V.; Daggett, V. J Mol Biol 2001, 305, 581–592.
9. Venkatachalam, C. M.; Urry, D. W. Macromolecules 1981, 14, 1225–1229.
10. Urry, D. W. J Prot Chem 1988, 7, 1–34.
11. Asakura, T.; Iwadate, M.; Demura, M.; Williamson, M. P. Int J Biol Macromol 1999, 24, 167–171.
12. Jelinski, L. W.; Sullivan, C. E.; Torchia, D. A. Nature 1980, 284, 531–534.
13. Sarkar, S. K.; Sullivan, C. E.; Torchia, D. A. Biochemistry 1985, 24, 2348–2354.
14. Saito, H.; Tabeta, R.; Shoji, A.; Ozaki, T.; Ando, I.; Miyata, I. Biopolymers 1984, 23, 2279–2297.
15. McMillian, R. A.; Conticello, V. P. Macromolecules 2000, 33, 4809–4821.
16. Urry, D. W. Methods Enzymol 1982, 82, 673–716.
17. Wishart, D. S.; Sykes, B. D.; Richards, F. M. J Mol Biol 1991, 222, 311–333.
18. Shoji, A.; Ando, S.; Kuroki, S.; Ando, I.; Webb, G. A. Annu Rep NMR Spectrosc 1993, 26, 55–98.
19. Saito, H.; Tuzi, S.; Naito, A. Annu Rep NMR Spectrosc 1998, 36, 79–121.
20. Wishart, D. S.; Sykes, B. D.; Richards, F. M. Biochemistry 1992, 31, 1647–1651.
21. Iwadate, M.; Asakura, T.; Williamson, M. P. J Biomol NMR 1999, 13, 199–211.
22. Havlin, R. H.; Le, H.; Laws, D. D.; deDios, A. C.; Oldfield, E. J Am Chem Soc 1997, 119, 11951–11958.
23. Walling, A. E.; Pargas, R. E.; deDios, A. C. J Phys Chem A 1997, 101, 7299–7303.
24. Tjandra, N.; Bax, A. J Am Chem Soc 1997, 119, 9576–9577.
25. Hong, M. J Am Chem Soc 2000, 122, 3762–3770.
26. Yao, X. L.; Hong, M. J Am Chem Soc 2002, 124, 2730–2738.
27. Hong, M.; Jakes, K. J Biomol NMR 1999, 14, 71–74.
28. Hong, M.; McMillan, R. A.; Conticello, V. P. J Biomol NMR 2002, 22, 175–179.
29. Castellani, F.; vanRossum, B.; Diehl, A.; Schubert, M.; Rehbein, K.; Oschkinat, H. Nature 2002, 420, 98–102.
30. Hong, M. J Magn Reson 1999, 136, 86–91.
31. Rienstra, C. M.; Hatcher, M. E.; Mueller, L. J.; Sun, B. Q.; Fesik, S. W.; Griffin, R. G. J Am Chem Soc 1998, 120, 10602–10612.
32. Hong, M.; Griffin, R. G. J Am Chem Soc 1998, 120, 7113–7114.
33. Hong, M. J Magn Reson 1999, 139, 389–401.
34. Gullion, T.; Schaefer, J. J Magn Reson 1989, 81, 196–200.

35. Liu, S. F.; Mao, J. D.; Schmidt-Rohr, K. J Magn Reson 2002, 155, 15–28.
36. Tycko, R.; Dabbagh, G.; Mirau, P. J Magn Reson 1989, 85, 265–274.
37. Bax, A.; Freeman, R.; Frankiell, T.; Levitt, M. H. J Magn Reson 1981, 43, 478–483.
38. Hong, M.; Yao, X. L. J Magn Reson, to appear.
39. Wishart, D. S.; Bigam, C. G.; Holm, A.; Hodges, R. S.; Sykes, B. D. J Biomol NMR 1995, 5, 67–81.
40. Spera, S.; Bax, A. J Am Chem Soc 1991, 113, 5490–5492.
41. Asakura, T.; Demura, M.; Date, T.; Miyashita, N.; Ogawa, K.; Williamson, M. P. Biopolymers 1996, 41, 193–203.
42. deDios, A. C.; Oldfield, E. J Am Chem Soc 1994, 116, 5307–5314.
43. Havlin, R. H.; Laws, D. D.; Bitter, H. L.; Sanders, L. K.; Sun, H.; Grimley, J. S.; Wemmer, D. E.; Pines, A.; Oldfield, E. J Am Chem Soc 2001, 123, 10362–10369.
44. deDios, A. C.; Pearson, J. G.; Oldfield, E. Science 1993, 260, 1491–1496.
45. Wishart, D. S.; Bigam, C. G.; Yao, J.; Abildgaard, F.; Dyson, H. J.; Oldfield, E.; Markley, J. L.; Sykes, B. D. J Biomol NMR 1995, 6, 135–140.
46. Wang, Y.; Jardetzky, O. Protein Sci 2002, 11, 852–861.
47. Creighton, T. E. Proteins: Structures and Molecular Properties; Freeman: New York, 1993.
48. Hong, M.; Gross, J. D.; Griffin, R. G. J Phys Chem B 1997, 101, 5869–5874.
49. Shoji, A.; Ozaki, T.; Fujito, T.; Deguchi, K.; Ando, I.; Magoshi, J. J Mol Struct 1998, 441, 251–266.
50. Simmons, A.; Rays, E.; Jelinski, L. W. Macromolecules 1994, 27, 5235–5237.
51. Ishida, M.; Asakura, T.; Yokoi, M.; Saito, H. Macromolecules 1990, 23, 88–94.
52. Beek, J. D. v.; Beaulieu, L.; Schafer, H.; Demura, M.; Asakura, T.; Meier, B. H. Nature 2000, 405, 1077–1079.
53. Vanderhart, D. L. J Magn Reson 1981, 44, 117–125.
54. Perry, A.; Stypa, M. P.; Tenn, B. K.; Kumashiro, K. K. Biophys J 2002, 82, 1086–1095.
55. Sun, H.; Sanders, L. K.; Oldfield, E. J Am Chem Soc 2002, 124, 5486–5495.